01

Dielectric barrier discharge in a low-pressure He−Ne mixture. Afterglow spectroscopy of $2p^5 5s \rightarrow 2p^5 3p$ transitions

© S.V. Gordeev, V. A. Ivanov¶, Yu. E. Skoblo

St. Petersburg State University,
198504 St. Petersburg, Russia

¶ e-mail: v.a.ivanov@spbu.ru

Received on January 27, 2022
Revised on January 27, 2022
Accepted on February 24, 2022

The results of a spectroscopic study and simulation of the processes of population and destruction of the levels of the $2p^5 5s$ configuration of a neon atom in a decaying plasma of a low-frequency barrier discharge in a He−Ne mixture are presented. Experimental conditions: helium pressure 0.08−22 Torr, neon pressure $\leq$ 3 mTorr, electron density less than 10^{11} cm^{-3}. On the basis of data on the evolution of the populations of the 3si levels (in Paschen's notation) with a change in helium pressure, data on the rate constants of collisional processes that determine the kinetics of these levels in He−Ne plasma are obtained more accurate than those available in the literature.

Keywords: dielectric barrier discharge, helium-neon plasma, excitation transfer, afterglow, inelastic collisions.

DOI: 10.21883/EOS.2022.05.54447.3208-21

Introduction

The dielectric barrier discharge (DBD) becomes more demanded for a wide range of applications in applied optics for optimization of the VUV radiation sources [1] and gas discharge lasers [2]. The properties of that discharge, such as operation within the region of pressures from two decimal places of Torr up to atmospheric one with minimum gas heating cause its application also in experimental practices for the study of elementary processes in weakly ionized plasma [3]. In this work, DBD is used as a source of He−Ne plasma in order to analyze the population kinetics of of excited levels of the neon atom of the $2p^5 5s$ configuration, which includes the upper laser levels to obtain data on the rate constants of inelastic collisions responsible for the formation of the properties of the active medium of the He−Ne laser. Despite the fact that hundreds of works [4] are devoted to these processes, the information on some of them is either estimative, or the data differ several times between one work and another. For example, cross-section of the excitation transfer in case of collisions

$$\mathrm{He}(2^1S_0) + \mathrm{Ne} \rightarrow \mathrm{He}(1^1S_0) + \mathrm{Ne}(3s_{3,4,5}) \qquad (1)$$

($3s_{2,3,4,5}$ — the levels the $2p^5 5s$ configuration in Paschen notations) according to the data of experiment [5] are less than 10^{-18} cm^2, which fails to correlate with the conclusions in [6]; with regard to the speed of one of the processes in active medium — collisional deactivation of upper laser level of the line 632.8 nm — discrepancies in the data are reaching three times [4]. One of the main reasons for these discrepancies lies in the unfortunate, in our opinion, choice of experimental conditions. The majority of works use plasma of gaseous discharge as the study object, having parameters similar to those in active medium, i.e. at a high temperature and density of electrons, sufficient for their participation, along with atoms, in the population of excited levels. Interpretation of the results of measurements of the rate constants of atomic processes under such conditions requires special analysis of the role of electrons [7]. Similar doubts arise with regard to the results that have been obtained at high densities of atoms: as noted in [6], reliable data on distribution of the population flows during the excitation transfer can be obtained only at the He−Ne mixture pressure of below 1 Torr. Therefore, low-frequency DBD seems to be an optimum way to create weakly ionized plasma, in the decay stage of which at close to room temperature of electrons and atoms in a wide range of pressures, starting from hundredths of Torr, it is convenient to observe the evolution of the densities of excited atoms in the framework of spectroscopic methods under changing conditions of the experiment.

Experimental part

We used simple scheme of implementation of the pulse barrier discharge (Fig. 1) of cylindrical configuration with electrodes on side faces of the discharge tube. Details concerning the discharge characteristics are described in the works [3,8]. Herein, the discharge frequency was 80−320 Hz, helium pressure varied from 0.08 to 22 Torr at the pressure of neon below 3 mTorr. The current of such discharge represents two half-waves of positive and negative polarity, with duration of several microseconds and the average value equal to zero. The latter is important, because unlike the direct current, there is no mixture separation due to cataphoresis in this discharge. Light fluxes were recorded using the method of multichannel photon counting with a resolution of 40 ns or more. The

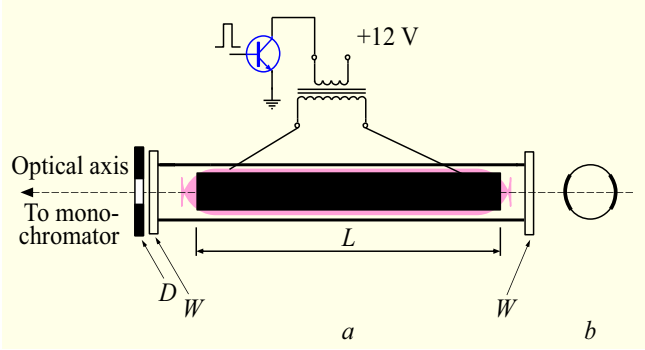

Figure 1. (*a*) Discharge tube — inner diameter of 3.9 cm, $L = 22$ cm; D — diaphragm with the diameter of 5 mm; W — quartz windows. (*b*) Location of electrodes on a side surface of the tube.

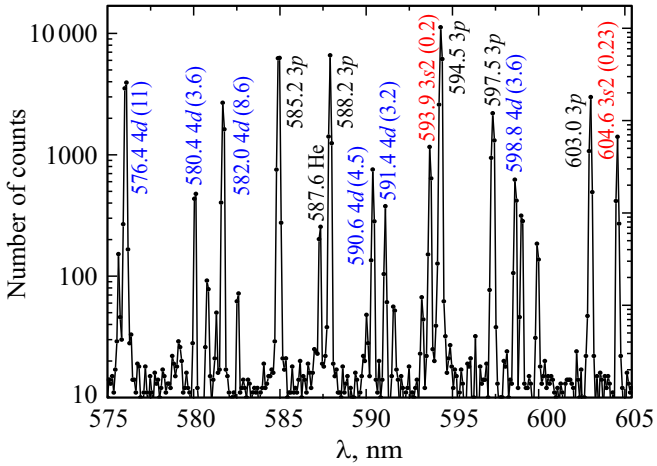

Figure 2. Fragment of the afterglow spectrum at the early stage of plasma decay. Pressure of helium is 0.66 Torr. The probabilities of transitions in 10^6 s^{-1} are given in parenthesis.

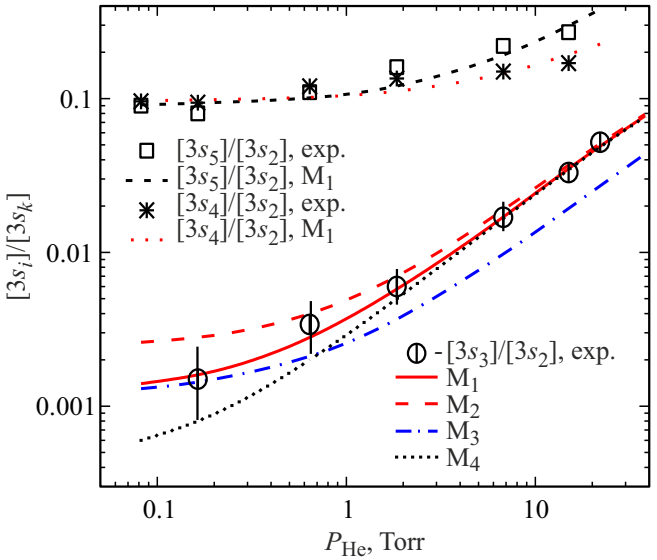

Figure 3. Experimental and model dependences of relative population of the levels $3s_i$ on helium pressure.

afterglow duration under any conditions was enough to observe the change of the mechanism of the $2p^5 5s$ levels population from the excitation transfer at the early stage of plasma decay to recombination of atomic Ne^+ or molecular $HeNe^+$ and Ne^{2+} ions with electrons [9,10]. The analysis of population levels was performed in the early afterglow, in which the intensities $J(t)$ of the spectral lines of the $5s \rightarrow 3p$ transitions fell identically to the density of the $[He(2^1S_0)(t)$ atoms For registration of $[He(2^1S_0)]$ we used the method absorption of the radiation of additional source on the line 501.6 nm In addition to the intensities of spectral lines $J(t)$ we registered the afterglow spectra. In this case the measurements were performed with the strobing of signal of photoelectron multiplier within the limits of the early afterglow.

Density of electrons at the early stage of the afterglow was evaluated based on the speed of falling of the density of atoms of helium $[He(2^1S_0)](t)$, whose main destruction channel in the conditions of low density of [Ne] is the process

$$He(2^1S_0) + e \xrightarrow{k_e} He(2^3S_1) + e. \qquad (2)$$

The rate constant (2) $k_e \sim 4 \cdot 10^{-7}$ cm^3/s, for the first time measured in [11], poorly depends on the temperature of electrons [12], varying during early afterglow. Under all experimental conditions at this stage, the time course $[He(2^1S_0)](t)$ coincided with the decrease of the line intensities of the $5s \rightarrow 3p$ transitions.

Discussion

Population of the levels $3s_2$ and $3s_3$

A fragment of afterglow spectrum is shown in Fig. 2. Comparatively low resolution in terms of the wavelengths is associated with small amount of light fluxes and the need for setting wide inlet and outlet slits of monochromator. The spectra within the region 570–670 nm were registered at the pressures of helium of 0.08, 0.16, 0.66, 1.85, 6.8, 15 and 22 Torr, out of which the first one was too low for confident registration of the lines emitted by the least populated [13] level $3s_3$. With regard to kinetics of that level, the data of the referred publication [4] are evaluative only, therefore, main attention herein was paid to it.

The results of the experiment on determination of relative population of levels $[3s_3]/[3s_2]$ are given in Fig. 3. These are obtained by averaging for the brightest lines J_{3sik} from each level $3s_i$:

$$[3s_i] = (1/N_k) \sum_k J_{ik}/S_{ik}A_{ik}.$$

Here $S_{ik}(\lambda)$ — the sensitivity of optical system of radiation registration, A_{ik} — probabilities of transitions, whose values were given from NIST Database [14], N_k —

the number of lines. As the values J_{3sik} we used the maxima of Gaussian functions, by using which we approximated the dependences $J(\lambda)$ within the registered spectra.

In Fig. 3 experimental data are given together with the results of simulation of the ratio of populations $[3s_3]/[3s_2]$. Vertical segments describe uncertainty of experimental values of intensities of the lines, which rises with the decrease of helium pressure as a result of decrease both relative, and absolute values of population of the level $3s_3$.

The model is built as follows. 1. Subject to the structure of the levels 3_{si} — two pairs ($3s_2$, $3s_3$ and $3s_4$, $3s_5$) of close levels with the gap between the pairs (within the scale of the energy ~ 0.086 eV), which considerably exceeds thermal energy, only collisional transitions between them were considered in the population balance $3s_2$ and $3s_3$, in addition to the excitation transfer:

$$\mathrm{Ne}(3s_2) + \mathrm{He} \leftrightarrow \mathrm{Ne}(3s_3) + \mathrm{He}. \qquad (3)$$

The ground for ignoring transitions from the levels $4d$ is their low population versus the level $3s_2$. It is clear from the comparison of intensities of the lines (Fig. 2) of transitions $4d \to 3p$ and $5s \to 3p$ subject to the fact that within the specified region of the spectrum, spectral sensitivity $S(\lambda)$ is changed insignificantly. Thus, population of the level $4d$ that emits the brightest line 576.4 nm in the afterglow (located 0.04 eV higher $3s_2$), is 13 times lower than that of $3s_2$, determined based on the line 593.9 nm.

The ratio of the rate constants of direct and inverse transitions (3) k_{23} and k_{32} is associated with the principle of detailed equilibrium, according to which

$$k_{32}/k_{23} = (g_2/g_3)\exp\{-0.006/kT_a\} \sim 2.4, \qquad (4)$$

g_2/g_3 is the ratio of statistical weights of the levels, $kT_a \sim 0.026$ eV at the room temperature of particles. The value of constant k_{23} was derived based on the condition of the best concordance of the model calculations with the experimental data.

2. The rate constants of the processes (1) of population of levels $3s_3$ and $3s_2$ in the model are bound by the coefficient m_3: $k_3^m = m_3 k_2^m$, as the constant k_2^m in the system of equations we used the value found based on the generally accepted [4] cross-section of the process $\langle\sigma_2\rangle = 3.6 \cdot 10^{-16}$ cm^2: $k_2^m = \langle\sigma_2\rangle\langle v\rangle$, where $\langle v\rangle$ is the average speed of colliding particles $\langle v\rangle \sim 1.4 \cdot 10^5$ cm/s at the temperature of atoms $T_a = 300$ K.

3. The destruction of populations considers transitions (3) and processes that are inverse the excitation transfer (1), whose rate constants were determined similar to (4) based on the detailed equilibrium principle. Therefore, the model includes two variable parameters: k_{23} and m_3.

4. The results of simulation depend on the degree of the radiation trapping during the transitions from the level $3s_2$ to ground state of the neon atom. Evaluations [15] based on the analysis of absorption at small pressures (neon pressure not to exceed 3 mTorr) for Doppler line shape (which is reasonable in our conditions at P_{He} not more than 22 Torr) show that the change of the transition probability introduced by the resonance trapping does not exceed 30%. Nevertheless, we performed calculations for both cases — $k_0R \ll 1$ and $k_0R \gg 1$ (k_0 is the coefficient of absorption in the center of the line, R is the radius of discharge tube).

Since characteristic times of change of populations in the experiment (in all conditions) exceed by orders of magnitude the radiation life times of excited states, the system of differential equations

$$\frac{d[3s_2]}{dt} = -[3s_2]\{A_2 + (k_{23} + k_{21})[\mathrm{He}]\} + k_{32}[3s_3][\mathrm{He}] + k_2^m[\mathrm{He}(2^1S_0)][\mathrm{Ne}], \qquad (5)$$

$$\frac{d[3s_3]}{dt} = -[3s_3]\{A_3 + (k_{32} + k_{31})[\mathrm{He}]\} + k_{23}[3s_2][\mathrm{He}] + m_3k_2^m[\mathrm{He}(2^1S_0)][\mathrm{Ne}] \qquad (6)$$

(A_2 and A_3 — sums of transition probabilities from the levels $3s_2$ and $3s_3$, k_{21} and k_{31} are the rate constants of inverse processes relative to excitation transfer to the levels $3s_2$ and $3s_3$) could be replaced with a system of algebraic equations (quasi-stationary approximation), based on which there is an obvious solution at $P_{\mathrm{He}} \to 0$:

$$\frac{[3s_3]}{[3s_2]}(0) = m_3\frac{A_2}{A_3}, \qquad (7)$$

i.e. the ratio rate constants of excitation transfer is determined by the ratio of populations at low pressure.

Model curves $\mathrm{M}_1-\mathrm{M}_4$ in Fig. 3 correspond to the following parameters.

M_1: $k_0R \ll 1$; $m_3 = 0.00037$, i.e. the cross-section of excitation transfer to the level $3s_3\langle\sigma_3\rangle = 0.00037\langle\sigma_2\rangle \sim 1.3 \cdot 10^{-19}$ cm^2; the second parameter of the model $k_{23} = 10^{-12}$ cm^3/s, which corresponds to the cross-section $\langle\sigma_{23}\rangle \sim 0.7 \cdot 10^{-17}$ cm^2.

M_2: $k_0R \ll 1$. For the test of the model sensitivity to change of the parameter m_3 we increased it two times: $m_3 = 0.00074$. First, we can see that this substitution virtually had no effect for the results of calculation at higher pressures of helium, and, second, subject to uncertainty of the experimental data, we may assume that the cross-section $\langle\sigma_2\rangle$ was determined with the error of about one and half times.

M_3: $k_0R \ll 1$. Check of the model sensitivity to change of the parameter k_{23}. $m_3 = 0.00037$ — the same as in M_1. Comparison of the curves M_1, M_2 and M_3, first, indicates that the determined value of one of the parameters of the model does not depend on the variation of another, and, second, uncertainty of the parameter k_{23} is much lower than the uncertainty m_3.

M_4: The only change compared to M_1 — $k_0R \gg 1$, i.e. the radiation at transitions to the ground state is completely trapped which three times decreases the probability of A_2 in the first equation of the model. As to be expected, the resonance trapping affects the results to a much

greater extent at low pressures when the role of collisional transitions is minor.

Summing up the possible sources of errors, including radiation trapping, we present the final results in the following form cross-section of the excitation transfer to the level $3s_3$ $\langle\sigma_3\rangle = (1.3 \pm {}^{0.8}_{0.5}) \cdot 10^{-19}\,\mathrm{cm}^2$, cross-section of collisional transition from the level $3s_2$ to the level $3s_3$ $\langle\sigma_{23}\rangle = (0.7 \pm 0.15) \cdot 10^{-17}\,\mathrm{cm}^2$. Note that with such ratio of the specified rate constants the main source of population of the level $3s_3$ in He−Ne plasma with the helium pressure over 1 Torr is collisional transition $3s_2 \to 3s_3$, but not the excitation transfer (1).

Compare these results with the few literature data. The work [6] states the lower limit of cross-section $\langle\sigma_3\rangle = 9 \cdot 10^{-19}\,\mathrm{cm}^2$, the authors of the work [5], as mentioned above, provided only evaluation of the cross-section of the excitation transfer to all three lower levels of the configuration $2p^5 5s$: $\langle\sigma_{3,4,5}\rangle$ below $10^{-18}\,\mathrm{cm}^2$. As regards $\langle\sigma_{23}\rangle$, we failed to find experimentally justified evaluations of the cross-section — probably, such an evaluation was obtained for the first time.

Populations of the levels $3s_4$ and $3s_5$

These levels are far more populated versus the $3s_3$, thus allowing to confidently register the emitted lines at minimum experimental pressure of helium 0.08 Torr. Size of symbols in Fig. 3 at $P_{\mathrm{He}} = 0.08$ Torr approximately reflect uncertainty of the ratios $[3s_4]/[3s_2]$ and $[3s_5]/[3s_2]$. It can be seen that these are poorly subject to the effect of collisional processes. The formula (7) is also relevant for them (with corresponding indices), by means of which and the data [14] on probabilities of transitions, having ignored trapping of resonance emission from the level $3s_4$, the following is obtained:

$$\frac{[3s_4]}{[3s_2]}(0) = m_4 \frac{A_2}{A_4} \sim \frac{[3s_5]}{[3s_2]}(0) = m_5 \frac{A_2}{A_5} \sim 0.09.$$

For the cross-sections of the excitation transfer, accordingly, we have $\langle\sigma_4\rangle \sim 0.11\langle\sigma_2\rangle = 4 \cdot 10^{-17}\,\mathrm{cm}^2$, $\langle\sigma_5\rangle \sim 0.028\langle\sigma_2\rangle = 10^{-17}\,\mathrm{cm}^2$ with the error associated with the statistics of measurements of the intensities of spectral lines, about 20%. With the pressure increase, as we can see from the data in Fig. 3, there are both increase of relative populations of both levels, and decrease of $[3s_4]/[3s_5]$. The first, as for the analysis $[3s_3]/[3s_2]$,, we associate with inclusion of collisional transitions $3s_2 \to 3s_{4,5}$. Change of the ratio $[3s_4]/[3s_5](P_{\mathrm{He}})$ may have two reasons: difference in cross-sections $\langle\sigma_{24}\rangle$ and $\langle\sigma_{25}$ and relaxation of populations due to collisional transitions $3s_4 \leftrightarrow 3s_5$ with approaching to equilibrium value $(g_4/g_5)\exp\{-0.011/kT_a\} \sim 0.4$ regardless of the ratio of cross-sections $\langle\sigma_{24}\rangle$ and $\langle\sigma_{25}\rangle$. This is why it is clear that the ratios $\langle\sigma_{24}\rangle/\langle\sigma_{25}\rangle$ and $\langle\sigma_{45}\rangle$, derived within the framework of the simple model in question (equations (5), (6) are added with similar ones for $3s_4$ and $3s_5$), appear to be dependent and cannot be unambiguously determined based on a limited set of experimental data used in the work. A rough estimate of cross-sections $\langle\sigma_{24}\rangle$ and $\langle\sigma_{25}\rangle$ can be obtained, having assumed that the efficiency of collisional „mixing" of levels $3s_4$ and $3s_5$ is the same as for $3s_2$ and $3s_3$: $\langle\sigma_{45}\rangle = \langle\sigma_{23}\rangle \sim 0.7 \cdot 10^{-17}\,\mathrm{cm}^2$. Model curves in Fig. 3 correspond to the cross-sections $\langle\sigma_{24}\rangle = 1.4 \cdot 10^{-17}\,\mathrm{cm}^2$ and $\langle\sigma_{25}\rangle = 2.3 \cdot 10^{-17}\,\mathrm{cm}^2$.

Conclusion

Spectroscopic study was performed on the spectrum of emission of the decaying plasma He−Ne within the range of change of density of atoms of helium [He] more than two order of magnitude and under the condition [Ne]≪[He]. Based on the comparison of the data on relative populations of the levels $3s_i$ (Paschen notations, $i = 2-5$) of the configuration $2p^5 5s$ of the atom of neon with the model calculations, we have found the rate constants of the excitation transfer to the levels $3s_3$, $3s_4$ and $3s_5$ during collision of atoms of helium in metastable state 2^1S_0 with atoms of neon and collisional transitions between the levels $3s_2$ and $3s_3$. This data can be used to refine theoretical models of processes in He−Ne plasma.

Conflict of interest

No conflict of interest.

References

[1] M.I. Lomaev, E.A. Sosnin, V.F. Tarasenko, D.V. Shits, V.S. Skakun, M.V. Erofeev, A.A. Lisenko. Instrum. Exp. Tech., **49** (5), 595−616 (2006). DOI: 10.1134/S0020441206050010

[2] U. Kogelschatz. Plasma Chem. Plasma Proc., **23** (1), 1−46 (2003). DOI: 10.1023/A:1022470901385

[3] V.A. Ivanov. Plasma Sources Sci. Technol., **29** (4), 045022 (2020). DOI: 10.1088/1361-6595/ab7f4c

[4] A.Z. Devdariani, A.L. Zagrebin, K. Blagoev. Annales de Physique, **17**(5), 365−470 (1992). DOI: 10.1051/anphys:01992001705036500

[5] J.T. Massey, A.G. Schulz, B.F. Hochheimer, S.M. Cannon. J. Appl. Phys., **36** (6), 658−659 (1965). DOI: 10.1063/1.1714054

[6] Yu.Z. Ionikh, N.P. Penkin. Opt. i spektr., **31** (5), 837−840 (1971) (in Russian).

[7] C.S. Willett, R.T. Young. J. Appl. Phys., **43** (2), 725−727 (1972). DOI: 10.1063/1.1661185

[8] V.A. Ivanov. Opt. Spectr., **126** (3), 167−172 (2019). DOI: 10.1134/S0030400X1903007X.

[9] V.A. Ivanov, A.S. Petrovskaya, Y.E. Skoblo. Opt. Spectr., **114** (5), 688−695 (2013). DOI: 10.1134/S0030400X13040097.

[10] V.A. Ivanov, A.S. Petrovskaya, Y.E. Skoblo. Russ. J. Phys. Chem. B, **9** (4), 565−570 (2015). DOI: 10.1134/S1990793115040235.

[11] A.V. Phelps. Phys. Rev.,**99** (4), 1307−1313 (1955). DOI: 10.1103/PhysRev.99.1307

[12] V.A. Ivanov, A.S Prikhod'ko, Yu.E. Skoblo. Opt. Spectrosc., **70** (3), 297−299 (1991).

[13] H.K. Haak, B. Wittig, F. Stuhl. Z. für Naturforsch. A, **35a** (12), 1342–1349 (1980). DOI: 10.1515/zna-1980-1214
[14] NIST Atomic Spectra Database Lines Form [Electronic source]. URL: https://physics.nist.gov/PhysRefData/ASD/lines_form.html
[15] H.K. Holt. Phys. Rev. A, **13** (4), 1442–1447 (1976). DOI: 10.1103/PhysRevA.13.1442